Available online at www.sciencedirect.com
ScienceDirect
Journal of Photochemistry and Photobiology A: Chemistry 183 (2006) 329–333
Journal of Photochemistry and Photobiology A:Chemistry
www.elsevier.com/locate/jphotochem

Nonlinear optical response of photonic bandgap structures containing PbSe quantum dots

Mikhail Haurylau [a,*], Jidong Zhang [a], Sharon M. Weiss [a,1], Philippe M. Fauchet [a], Dmitri V. Martyshkin [b], Valery I. Rupasov [b], Sergei G. Krivoshlykov [b]

[a] *University of Rochester, Department of Electrical and Computer Engineering, Rochester, NY 14627, United States*
[b] *ALTAIR Center, LLC 1 Chartwell Circle, Shrewsbury, MA 01545, United States*

Available online 30 March 2006

Abstract

New nanocomposite materials with large optical nonlinearity are important for the development and miniaturizing of active components and integrated circuits for all-optical signal processing and computing. To enable on-chip integration with silicon microelectronics nonlinear signal processing components compatible with silicon nanophotonics need to be developed. In this paper, we study the nonlinear optical response of silicon-based photonic bandgap (PBG) structures filled with PbSe quantum dot (QD) materials and experimentally demonstrate the feasibility of a new class of nonlinear nanophotonic devices for all-optical signal processing based on such microstructures. Active tuning is demonstrated for both out-of-plane components, with one-dimensional porous silicon PBG microcavities and in-plane components, using one-dimensional PBG waveguide-based microresonators.

Keywords: PbSe; Quantum dots; Nanophotonics; Photonic bandgap; Silicon photonics

1. Introduction

Quantum dots (QDs) made of IV–VI semiconductors such as PbSe have recently attracted much attention due to their large optical nonlinearity and potential applications in photonic devices [1]. These QDs offer access to the regime of strong quantum confinement, which results in enhanced electronic and optical properties [2]. Such properties can be used to create optical devices with functionalities that have not been possible previously.

An important optical platform for high-performance ultra-compact optical elements is a silicon-based photonics [3–5]. It offers superior fabrication capabilities and integration with existing microelectronic circuits. Unfortunately, silicon does not exhibit large optical nonlinearity. In this work to allow for all-optical switching we infiltrate silicon-based photonic devices with nonlinear PbSe QDs. Silicon-based photonic bandgap (PBG) structures are used to concentrate the electromagnetic field inside the QD material in order to utilize their nonlinear properties.

2. Experimental

Both out-of-plane and in-plane PBG components were fabricated. The out-of-plane PBG components were fabricated with porous silicon [6]. Porous silicon is produced by electrochemical etching in a hydrofluoric acid-based electrolyte. The one-dimensional porous silicon PBG microcavities were formed on 0.01 Ω cm p-type (1 0 0) silicon in a solution of 15% hydrofluoric acid in ethanol. In order to create the periodic refractive index profile necessary for PBG structures, an sequential current density of 5 mA/cm^2 for 39 s and 50 mA/cm^2 for 9 s was applied during etching, to form a Bragg mirror with layers of 50 and 75% porosity [7]. A microcavity was created by etching a defect layer between two Bragg mirrors using a current density of 50 mA/cm^2 for 19 s. The porous silicon created by this etching procedure is mesoporous silicon with an average pore diameter of 20–50 nm, much less than a wavelength of the infrared light. Therefore, the refractive index of each layer of the microcavity can be calculated by the Bruggeman effective medium approximation [8]. The refractive index of porous

* Corresponding author. Tel.: +1 585 275 1252; fax: +1 585 275 2073.
E-mail address: haurylau@ece.rochester.edu (M. Haurylau).
1 Present address: Department of Electrical Engineering and Computer Science, Vanderbilt University, United States.

1010-6030/$ – see front matter © 2006 Elsevier B.V. All rights reserved.
doi:10.1016/j.jphotochem.2006.03.026

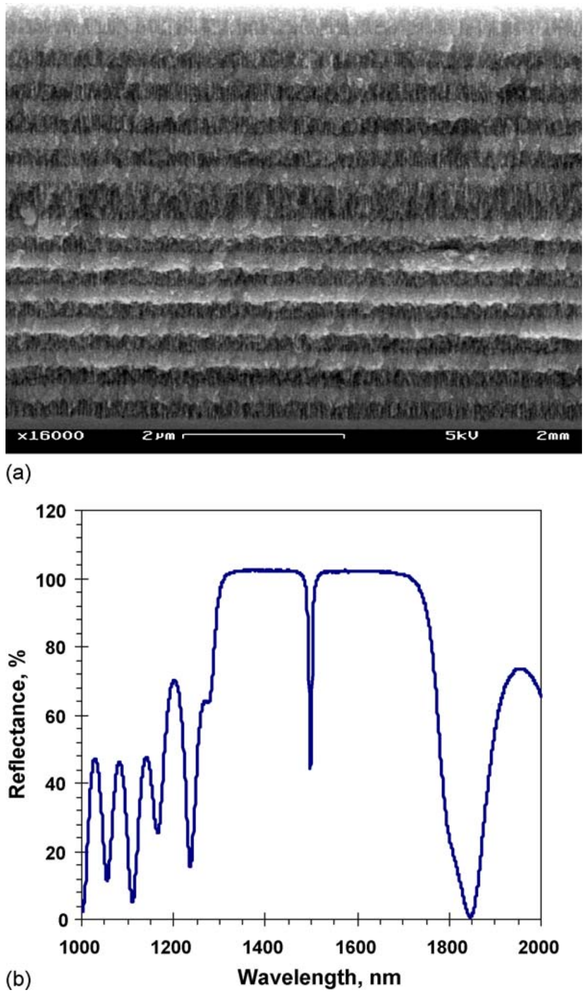

Fig. 1. (a) SEM image of porous silicon one-dimensional PBG microcavity. The air interface is at the top and the silicon interface is at the bottom of the image. The microcavity consists of a 5.5 period upper Bragg mirror with alternating 50 and 75% porosity one-quarter-wavelength optical thickness layers, a central 75% porosity one-half-wavelength optical thickness defect layer and a six-period lower Bragg mirror. (b) Experimentally measured reflectance spectrum of porous silicon one-dimensional PBG microcavity.

silicon decreases as the porosity increases. Near the resonance wavelength, the refractive indices of the 50 and 75% porosity layers are 2.15 and 1.43, respectively. The geometry of the porous silicon PBG microcavity structure was developed and optimized using a custom-built simulation code based on the transfer matrix method. The cross-sectional image of the resulting microcavity is illustrated in Fig. 1a. The defect layer in the center of the structure breaks up the perfect periodicity of the refractive index profile and creates a narrow passband within the high reflectance region, as shown in Fig. 1b. Good agreement was achieved between the simulation and experiment for the QD infiltrated microcavity.

Fabrication of in-plane PBG structures involves various nanofabrication techniques, including electron-beam beam lithography and reactive ion etching (RIE). We chose the silicon on insulator (SOI) platform in which the silicon "device" layer serves as a guiding region while the buried silicon dioxide layer is used as a lower index cladding. The advantage of this platform is in the high refractive index contrast between the light guiding layer and the surrounding regions, which allows for a high degree of mode confinement and thus superior optical performance.

First electron-beam lithography was used to define the PBG structure topography with typical dimensions of 100 nm. Because of the insufficient process selectivity between the resist material and silicon, a sacrificial silicon dioxide layer was used as a mask for the RIE of silicon. A chlorine-based plasma was used for the dry etching of the silicon layer. The fabrication process and an SEM image of an SOI-based microresonator are depicted in Fig. 2. As with the out-of-plane porous silicon microcavity, a defect layer in the center of the in-plane waveguide-based structure creates a narrow passband within the high reflectance region. While the refractive index contrast in the previous case was achieved by using layers with different porosities, in the SOI-based microresonator the Bragg mirrors are defined by placing air holes inside the silicon waveguide. The electromagnetic field is enhanced inside the smaller hole that is part of the defect layer [9]. This hole can be infiltrated with active materials. To develop the waveguide-based PBG microresonator, the full-vectorial 3D finite-difference time domain (FDTD) simulation software "R-soft Fullwave" was used [10].

After the fabrication, the nonlinear PbSe QD material was infiltrated inside the fabricated silicon PBG structures. Optical characterization of out-of-plane porous silicon PBG microcavities was performed in the reflection mode using a broadband light source for the 1500–1600 nm spectral region or a tungsten-halogen light source for the 1300–1400 nm spectral region and an optical spectrum analyzer (Ando, AQ-6310B). The in-plane waveguide-based PBG microresonators were characterized in the transmission mode using the broadband light source and the optical spectrum analyzer. Microscope objectives were used to couple the probe light into one side of an SOI waveguide and collect light from the other side. The radiation of an argon-ion laser operating in a multiline mode (514, 488 and 457 nm), was used to pump both types of PBG microresonators. A laser power of 50 mW was focused to a spot of about 200 μm in diameter. The schematics of the out-of-plane and in-plane measurement setups are illustrated in Fig. 3a and b, respectively.

3. Results and discussion

3.1. PbSe nonlinear quantum dot material

The all-optical PBG components developed in this work take advantage of the large nonlinearity of the PbSe QD material. It has been demonstrated in recent experiments using the Z-scan technique that PbSe QDs in toluene exhibit extraordinarily large nonresonant nonlinear index $n_2 = 5.5 \times 10^{-5}$ esu ($n = n_0 + (n_2/2)|E|^2$) with a response time faster than 10 ns [11]. Such a large nonlinearity has been attributed to a thermal mechanism due to efficient light absorption in PbSe QDs. The large surface-to-volume ratio of these QDs produce a fast heat transfer to the toluene matrix having large dn/dT. A theoretical estimate based on this model gives a nonlinear index change normalized

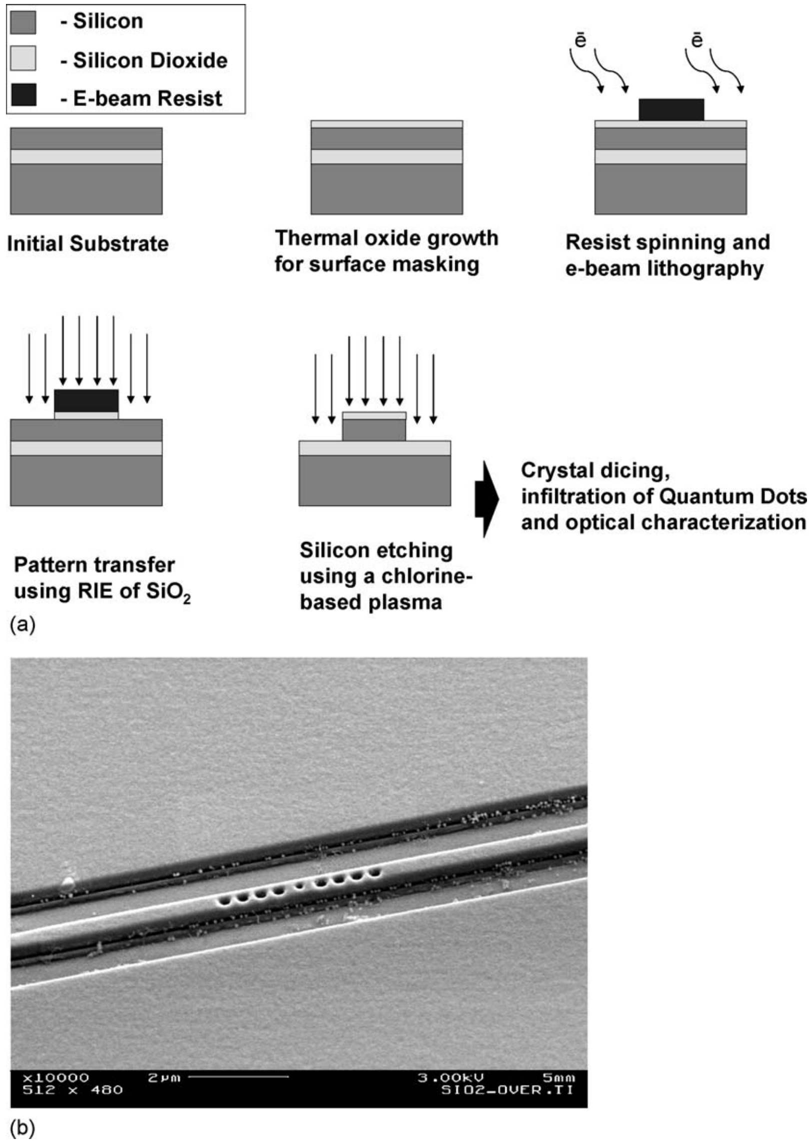

Fig. 2. (a) Outline of the fabrication of an SOI waveguide-based PBG microresonator. (b) Plan view of an SOI in-plane PBG waveguide microresonator. The microresonator consists of two four-layer Bragg mirrors defined by the circular holes in the silicon waveguide. A small hole in the middle of the defect layer is used for electromagnetic field enhancement inside the QD material.

by pumping intensity of $\Delta n/I = -0.9 \times 10^{-7}$ cm^2/W which is in a good agreement with the experimental results.

3.2. Measurement of the all-optical tuning of PBG structures

In this work, porous silicon PBG microcavities are used to modulate optical signals out-of-plane while waveguide-based PBG structures provide in-plane light modulation. Optical pumping changes the absorption coefficient and thus the refractive index of the QD material. Therefore, pumping also leads to a modulation of the optical properties of the PBG structures.

Fig. 4a shows an experimental measurement of the resonance frequency tuning that is achieved by pumping the one-dimensional porous silicon PBG microcavity. The resonance shifts due to the nonlinear optical effect in PbSe QD material infiltrated in porous silicon matrix and is reversible when the pumping is turned off. PbSe absorption of the pump beam increases the QD temperature, which is followed by a rapid thermal energy transfer to the surrounding toluene matrix. Because of the large negative dn/dT of the toluene, the effective refractive index of the QD material decreases. This change shifts the resonance frequency of the microcavity to *shorter* wavelengths by more than 3 nm. To verify that this effect is due to the QD material itself, a control experiment was conducted with an empty porous silicon PBG microcavity. The resulting spectrum shown in Fig. 4b indicates a shift to *longer* wavelengths, i.e. the opposite direction to the sample infiltrated with QDs. The redshift of the control sample is due to the heating of the empty porous silicon matrix by the incident pump beam, because of the positive dn/dT in porous silicon [12].

A similar experiment of the in-plane all-optical PBG switching is illustrated in Fig. 5a. The nonlinear optical effect in the QD material shifts the resonance frequency of the microcavity

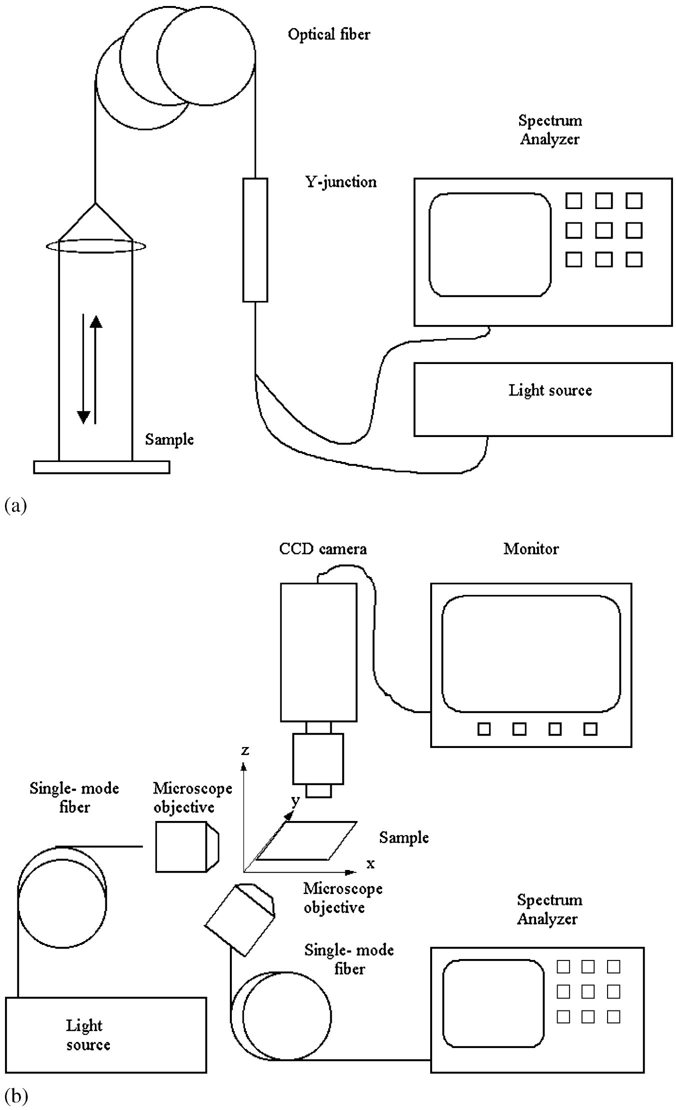

Fig. 3. (a) Optical setup for characterization of out-of-plane porous silicon PBG microcavities in the reflection mode. A broadband light source is used to illuminate the microcavity using a fiber probe and an optical spectrum analyzer is used to measure the reflectance spectrum. (b) Optical setup for characterization of the in-plane waveguide-based PBG microresonators in the transmission mode. Microscope objectives are used to couple the probe light into one side of an SOI waveguide and collect light from the other side. An argon-ion laser was used to pump both types of devices.

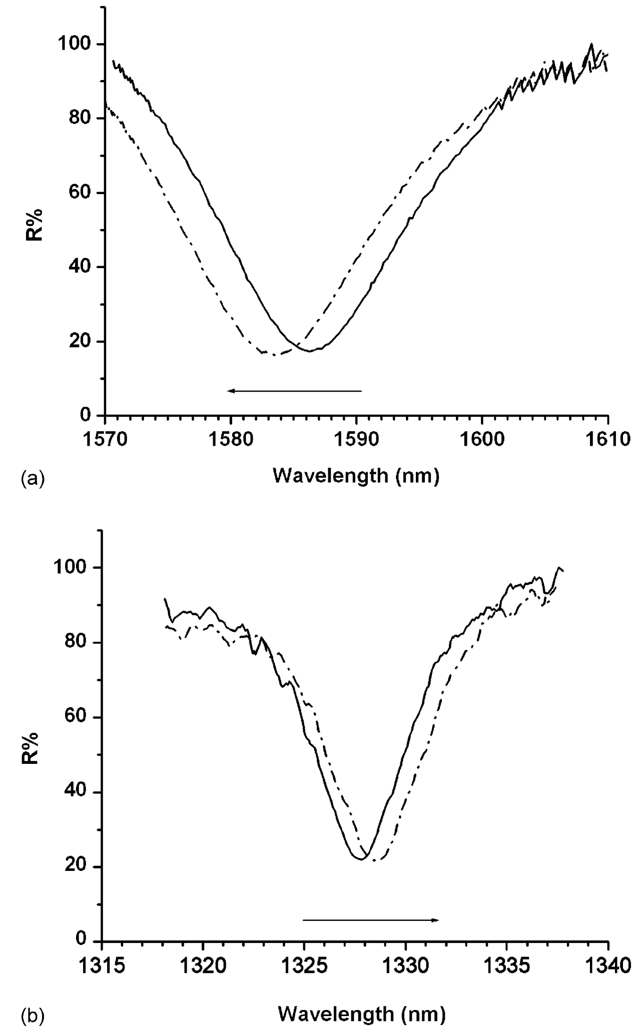

Fig. 4. (a) Influence of pumping on the reflectance spectrum of a porous silicon one-dimensional PBG microcavity containing PbSe QD material. Near the resonance frequency, a large contrast in reflectance is observed. (b) Spectrum measured in the control experiment using an empty porous silicon one-dimensional PBG microcavity. The redshift of the resonance is associated with thermal heating of the silicon backbone and is due to the temperature dependence of the refractive index of silicon. In both figures, the solid lines represent sample spectra without optical pumping, and the dash–dot lines represent spectra under optical pumping.

to *shorter* wavelengths by 3 nm. Consequently, for incident light near the resonance frequency, a contrast in transmittance as high as three to two can be achieved. In the control experiment with a toluene infiltrated PBG structure that does not contain QDs, optical pumping did not shift the resonance position (Fig. 5b).

The contrast between the optical signal level at the resonance wavelength and the stopband is critical to the efficient operation of the microresonator-based all-optical switch. The sharper the resonance, the easier it is to transition between the off- and on-states of the device. Higher switching contrasts can be achieved by utilizing resonators with higher quality factors. The quality factor of the QD infiltrated porous silicon microcavity was likely limited by the measurement setup. While the 1D porous silicon microcavity was optimized to operate with a normal incident light, the angular light dispersion from the fiber probe results in the broadening of the resonance peak. The quality factor of the SOI-based waveguide microresonator was limited by diffraction losses from the resonant cavity. The quality factor can be significantly increased by using 2D PBG structures [13].

Capitalizing on these results, a conceptual design of all-optical signal processing components enabling on-chip integration with silicon microelectronics can be proposed. In the first step, mainstream silicon microelectronics processing is used to create passive optical silicon structures that can be integrated with CMOS electronic devices. In the second step, the backbone silicon structures are infiltrated with active nonlinear optical materials to enable all-optical switching. This approach allows combining the technological advantages of CMOS electronics with the flexibility and superior optical properties of such non-

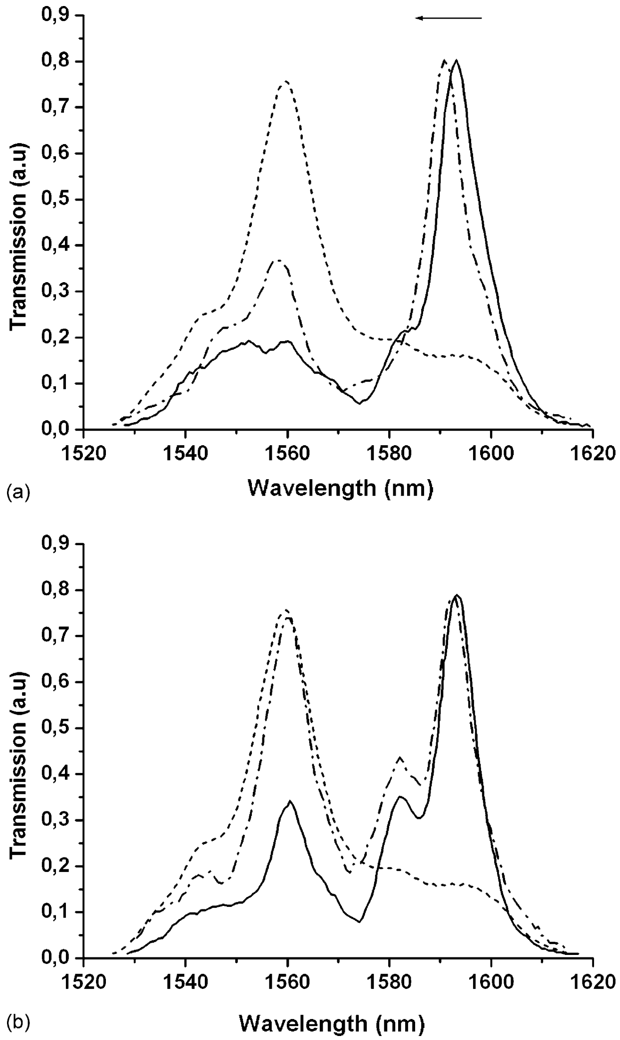

Fig. 5. (a) Influence of pumping on the optical spectrum of waveguide-based silicon PBG microresonator containing PbSe QD material. The background spectrum was measured in transmission through an identical waveguide without PBG structure. The transmission peak at 1560 nm is an artifact due to the emission spectrum of the light source. The peak associated with PBG microresonator is located near 1590 nm. Note the blueshift of the resonance peak near 1590 nm, associated with the large third-order nonlinearity of the QD material. (b) Spectra measured in the control experiment with a silicon PBG microresonator infiltrated with toluene. Dotted lines, background spectra; solid lines, sample spectra without optical pumping; dash–dot lines, sample spectra with optical pumping.

linear materials as PbSe QDs. A number of novel structures can be designed with this approach, such as all-optical transistors, nonlinear Fabry–Perot cavities, optical memory/switches and tunable filters.

4. Conclusions

A new class of nonlinear nanophotonic devices for all-optical signal processing is experimentally demonstrated by using silicon-based photonic bandgap structures infiltrated with PbSe quantum dot materials. Two possible implementations of the nonlinear photonic bandgap microstructure have been studied. The first one is based on porous silicon photonic bandgap microcavities. The second one is a nonlinear photonic bandgap structure with a defect implemented in a silicon-on-insulator waveguide. Both fabricated photonic bandgap structures demonstrated an extraordinarily large nonlinear optical response due to the large nonlinearity of the PbSe quantum dot material ($n_2 = 5.5 \times 10^{-5}$ esu). A new class of all-optical devices can be designed with this approach, which allows combining the advantages of silicon microelectronic processing with the flexibility of a wide range of nonlinear optical materials.

Acknowledgements

Financial support from the US Air Force, Contract FA9550-04-C-0090 is gratefully acknowledged. This work was performed in part at the Cornell Nanoscale Facility, a member of the National Nanotechnology Infrastructure Network, which is supported by the National Science Foundation (Grant ECS 03-35765).

References

[1] Y.K. Olsson, G. Chen, R. Rapaport, D.T. Fuchs, V.C. Sundar, J.S. Steckel, M.G. Bawendi, A. Aharoni, U. Banin, Appl. Phys. Lett. 85 (19) (2004) 4469.
[2] A.L. Efros, A.L. Efros, Sov. Phys. Semicond. 16 (1982) 772.
[3] A. Birner, R.B. Wehrspohn, U.M. Gösele, K. Busch, Adv. Mater. 13 (2001) 377.
[4] S.M. Weiss, H. Ouyang, J. Zhang, P.M. Fauchet, Opt. Express 13 (2005) 1090.
[5] M. Haurylau, A.R. Shroff, P.M. Fauchet, Phys. Status Solidi A 202 (8) (2005) 1477.
[6] P.M. Fauchet, Encyclopedia of Applied Physics, Update 2, Wiley-VCH, Verlag, 1999, p. 249.
[7] S.M. Weiss, P.M. Fauchet, Phys. Status Solidi A 197 (2003) 556.
[8] W. Theiss, Surf. Sci. Rep. 29 (1997) 91.
[9] B. Schmidt, V. Almeida, C. Manolatou, S. Preble, M. Lipson, Appl. Phys. Lett. 85 (21) (2004) 4854.
[10] www.rsoftdesign.com.
[11] V.I. Rupasov, I.S. Moskalev, D.V. Martyshkin, S.G. Krivoshlykov, Final Report on MDA/NAVY Phase II Contract N00178-03-C-1058.
[12] S.M. Weiss, M. Molinari, P.M. Fauchet, Appl. Phys. Lett. 83 (10) (2003) 1980.
[13] B. Maune, M. Loncar, J. Witzens, M. Hochberg, T. Baehr-Jones, D. Psaltis, A. Scherer, Y.M. Qiu, Appl. Phys. Lett. 85 (3) (2004) 360.